Mon. Not. R. Astron. Soc. **338,** 147–155 (2003)

The new model of a tidally disrupted star: further development and relativistic calculations

P. B. Ivanov,[1,4⋆] M. A. Chernyakova[2,4,5] and I. D. Novikov[3,4,6,7]

[1] *School of Mathematical Sciences, Queen Mary, University of London, Mile End Road, London E1 4NS*
[2] *Integral Science Data Center, Chemin d'Ecogia 16, CH-1290 Versoix, Switzerland*
[3] *Theoretical Astrophysics Center, Juliane Maries Vej 30, DK-2100 Copenhagen, Denmark*
[4] *Astro Space Center of PN Lebedev Physical Institute, 84/32 Profsoyuznaya Street, Moscow, 117810, Russia*
[5] *Geneva Observatory, CH-1290, Sauverny, Switzerland*
[6] *University Observatory, Juliane Maries Vej 30, DK-2100 Copenhagen, Denmark*
[7] *NORDITA, Blegdamsvej 17, DK-2100, Copenhagen, Denmark*

Accepted 2002 September 1. Received 2002 August 20; in original form 2002 May 5

ABSTRACT

In this paper we develop a new semi-analytical model of a tidally perturbed or tidally disrupted star proposed recently by two of us. This model is effectively a one-dimensional Lagrangian model and it can be evolved numerically much faster than the conventional three-dimensional (3D) models. A self-consistent derivation of dynamical equations of the model is performed and several important theorems concerning the dynamics of the model are proved without any particular assumptions concerning the equation of state of the stellar gas. The dynamical equations are solved numerically for the case of an $n = 1.5$ polytropic star evolving in the relativistic tidal field of a 10^7-$M_\odot$ Kerr black hole. Some results of these calculations are compared with the results of calculations based on finite-difference 3D simulations. The comparison shows a very good agreement between both approaches to the problem. Then we show that the strength of the tidal encounter depends significantly on the relative orientation of the orbital angular momentum of the star and the spin of the black hole.

Key words: black hole physics – galaxies: nuclei.

1 INTRODUCTION

This paper continues the study of a new dynamical model of a star evolving under the influence of a tidal field. This semi-analytical model has been proposed by two of us in a recent paper Ivanov & Novikov (2001, hereafter IN). It allows researchers to calculate the outcome of a strong tidal encounter of a star with the source of a tidal field much faster than the standard three-dimensional (3D) approach, and evolves the star under the influence of a tidal field over a much longer time. On the other hand, testing of the model for the case of a Newtonian tidal field of a point mass has shown that the new model gives very good quantitative agreement with the results of three-dimensional simulations. Therefore, the new model could be used in a situation where the formulation of a problem demands many different computations of the tidal encounter events with different parameters, or for calculating the stellar evolution in a complicated tidal field, and where the present-day 3D simulations cannot be used owing to problems with computational time or other problems.[1] A natural example of such a problem is an attempt to survey the parameter space of the problem of tidal disruption of stars by a Kerr black hole.

The main feature of the new model consists of an assumption concerning the motion of the stellar gas perturbed by the action of a tidal field. Namely, it is assumed that different mass shells of the star always keep the shape of ellipsoids during the evolution of the star in the tidal field.[2] This assumption allows us to reduce the complicated non-linear three-dimensional dynamics of the stellar gas to an effectively one-dimensional Lagrangian numerical scheme. The dynamical equations of our model are derived from the so-called virial relations written for each mass shell (see the next section), and form a set of non-linear one-dimensional partial differential equations of

[1] See IN for an overview of works on tidal encounters and astrophysical applications.

[2] Therefore the model is a direct generalization of the so-called affine model of the star (Carter & Luminet 1982, 1983, 1985; Lattimer & Schramm 1976), which has been used intensively for investigation of the tidal encounters prior to the development of modern 3D computational methods. However, in contrast to the affine model, the different elliptical mass shells evolve differently, with different parameters and orientations.

⋆E-mail: p.ivanov@qmul.ac.uk

hyperbolic type coupled with the tidal field. They depend on time and a Lagrangian variable that could be represented by the mass enclosed within a particular shell or the radius of the shell in the unperturbed spherical state of a star.

There is one fundamental drawback in the variant of the model studied by IN. Namely, the 'thermal terms' (i.e. the terms determined by the gas energy and pressure) in the virial relations were treated by IN in an approximate manner. This led to unphysical behaviour of the model – the mass shells corresponding to different Lagrangian radii were allowed to intersect each other during the evolution of the star. Therefore, a variant of IN was not suitable for studying the density, pressure and velocity distribution within the star. However, the distribution of these quantities represents a significant interest in the problems connected with the problem of tidal disruption. For example, one would need to know these quantities for a study of the subsequent evolution of the gas liberated from the star after a fly-by of a black hole and the formation of an accretion disc (or torus). The main purpose of this paper is to resolve this difficulty of the model. In this paper, we calculate the 'thermal terms' exactly and derive the dynamical equations of our model in a self-consistent way (see the next section). Then, we apply our advanced variant of the model to the problem of a fly-by of an $n = 1.5$ polytropic star around a Kerr black hole. We test the model against three-dimensional calculations made by Diener et al. (1997) for the same problem and the same parameters. We find very good agreement between our calculations and the calculations based on the 3D approach.

Our paper is organized as follows. We derive the dynamical equations of our model in the next section. In Section 3 we discuss the results of numerical simulations. A discussion and conclusions are presented in Section 4. The paper is written in a self-consistent way, and all important relations are derived in the text without referring to IN.

Following IN we use an unusual summation convention: summation is performed over all indices appearing in our expressions more than once but summation is not performed if indices are enclosed in parentheses. Bold letters represent matrices in abstract form. All indices can be raised or lowered with help of the Kronecker delta symbol, but we distinguish between the upper and lower indices in order to enumerate the rows and columns of matrices, respectively.

2 DERIVATION AND ANALYSIS OF THE DYNAMICAL EQUATIONS

We derive and analyse dynamical equations of our model in a manner similar to that described in our previous paper (IN). However, as we mention in the introduction, we do not use simplifying assumptions concerning 'thermal terms' in our equations (for the exact definition of the thermal terms, see equations 15–19 below). Also, we prove several important theorems concerning the dynamics of our model without any particular assumptions concerning the equation of state of the stellar gas.

At first, we would like to introduce coordinate systems and several useful kinematical quantities. We use two different coordinate systems: (i) Cartesian coordinates x^i associated with a locally inertial frame centred at the geometrical centre of the star (we call those below 'the Eulerian coordinates' of the gas element); (ii) Cartesian coordinates x_0^i of the gas elements in an unperturbed spherical state of the star (say, before the star is deformed by the tidal field). By definition, these coordinates are not changing during the evolution of any particular gas element, and therefore below we call them 'the Lagrangian coordinates'. As we have mentioned in the introduction, we assume that the star consists of elliptical shells, and these shells are not deformed during the evolution of the star. This assumption allows us to write the transformation law between the Lagrangian and Eulerian coordinates in the form:

$$x^i = T^i_j(t, r_0) e^j_0, \tag{1}$$

where $r_0 = \sqrt{x_{0i} x^i_0}$ is the Lagrangian radius of a particular shell, and $e^i_0 = x^i_0 / r_0$ are direction cosines in the Lagrangian space ($e_{0i} e^i_0 = 1$). We represent the position matrix $\mathbf{T}$ and its inverse $\mathbf{S}$ as a product of two rotational matrices $\mathbf{A}$ and $\mathbf{E}$, and a diagonal matrix $\mathbf{B}$:

$$T^i_j = A^i_l B^l_m E^m_j = a_l A^i_l E^l_j, \quad S^i_j = a_l^{-1} A^j_l E^l_i, \tag{2}$$

where $B^l_m = a_{(l)} \delta^{(l)}_m$ and a_l are the principal axes of the elliptical shell. The Jacobian $D = |\partial x^i / \partial x^j_0|$ of the mapping between the Lagrangian and Eulerian spaces can be written as

$$D\left(x^i_0\right) = \frac{g e_{0l} e_{n0} R^{\ln}}{r_0^2}, \tag{3}$$

where

$$g = |\mathbf{T}| = a_1 a_2 a_3, \tag{4}$$

is the determinant of the matrix $\mathbf{T}$, and the symmetric matrix $R^{\ln}$ determines a local shear and a change of volume of the neighbouring shells:

$$R^{\ln} = \frac{1}{2}\left[S^l_m \left(T^m_n\right)' + S^n_m \left(T^m_l\right)'\right], \tag{5}$$

with the primes denoting differentiation with respect to r_0.[3] The matrix $\mathbf{R}$ can be represented in terms of its eigenvalues f_m and the rotational matrix $\mathbf{O}$:

$$R^{\ln} = f_m O^l_m O^n_m. \tag{6}$$

As it follows from the law of mass conservation, the evolution of the gas density ρ is determined by the evolution of D:

$$\rho(t, x^i) = \frac{\rho_0(r_0)}{D}, \tag{7}$$

where $\rho_0(r_0)$ is the gas density in the unperturbed spherical state of the star. If one of the eigenvalues f_m goes to zero, the density $\rho(t, x^i)$ goes to infinity at a certain value of x^i_0. This corresponds physically to the intersection of two neighbouring shells. However, we assume that pressure forces can always prevent the shells from intersecting, and therefore the eigenvalues f_m are always positive.

Similar to IN, we start the derivation of the dynamical equation of our model from the integral consequences of the exact hydrodynamical equations: the equation of energy conservation and the so-called virial relations. We write the energy conservation equation in the adiabatic approximation, thus neglecting the energy transfer between neighbouring shells, the entropy generation arising from nuclear reactions, viscosity, etc.,

$$\frac{\mathrm{d}}{\mathrm{d}t}\left[\int \mathrm{d}^3x(\rho v^2/2 + \epsilon) + \mathcal{P}\right] = -\int \mathrm{d}S_i\,(p v^i) + \int \mathrm{d}^3x\left(\rho C_{ij} v^i x^j\right). \tag{8}$$

Here v^i is the velocity of the gas element, $v = \sqrt{v_i v^i}$, p is the pressure and ϵ is the energy density per unit volume. $\mathcal{P}$ denotes the potential energy of the star. The matrix C^i_j represents the tidal tensor, and

[3] Note a useful formula for the averaged value of the Jacobian D (IN): $\bar{D} = (1/4\pi)\int \mathrm{d}\Omega\, D = \mathrm{d}g/\mathrm{d}r_0^3$. Here integration is performed over a unit sphere in the Lagrangian space.

therefore it is symmetric and traceless. The virial relations have the form

$$\frac{\mathrm{d}}{\mathrm{d}t}\int \mathrm{d}^3x\,(\rho x^k v^i) = \int \mathrm{d}^3x\,(\rho v^k v^i) + \delta^{ki}\int \mathrm{d}^3x\,p - \int \mathrm{d}S_i\,(x^k p) + \mathcal{P}^{ki} + \int \mathrm{d}^3x\left(\rho C^i_j x^k x^j\right), \tag{9}$$

where $\mathcal{P}^{ki}$ is the so-called potential energy tensor:

$$\mathcal{P}^{ki} = -\frac{1}{2}\int \mathrm{d}^3x \int \mathrm{d}^3x_1\,\rho(x^i)\rho\left(x^i_1\right)\frac{\left(x^k - x^k_1\right)\left(x^i - x^i_1\right)}{|\boldsymbol{x}-\boldsymbol{x}_1|}. \tag{10}$$

Obviously, we have $\mathcal{P} = \mathcal{P}^{kk}$.

Now we substitute the evolution law (1) in equations (9) and calculate all terms in these equations. Then, differentiating the result with respect to the Lagrangian mass coordinate

$$M(r_0) = 4\pi\int_0^{r_0}\rho_0(r_1)\,\mathrm{d}r_1 \tag{11}$$

we obtain the dynamical equations of our model [below we use the mass $M(r_0)$ of the gas inside the shell of radius r_0 as a new Lagrangian coordinate instead of r_0]. Analogously, we obtain a differential form of the law of energy conservation from the integral form (8).

We calculate explicitly 'gravitational' parts of equations (8) and (9) (the potential energy and potential energy tensor) making an additional simplifying approximation. Namely, we assume that the gravitational force acting on the gas near the shell with some Lagrangian radius r_0 is equivalent to the gravitational force of a uniform density ellipsoid with a mass equal to the part of the mass of the star within that shell. The principal axes of that ellipsoid coincide with the principal axes of the shell, and the density is averaged over the volume enclosed in the shell. Under this assumption the 'averaged' potential energy tensor $\bar{\mathcal{P}}^{ik}$ has the form

$$\bar{\mathcal{P}}^{ik} = -\frac{1}{2}\int \mathrm{d}M\,GMA^i_jA^k_j\frac{a_j^2D_j}{g}, \tag{12}$$

and the 'averaged' potential energy $\bar{\mathcal{P}} = \bar{\mathcal{P}}^{kk}$ is

$$\bar{\mathcal{P}} = -\frac{1}{2}\int \mathrm{d}M\,GM\frac{a_j^2D_j}{g}. \tag{13}$$

The dimensionless quantities D_j have been described in, for example, Chandrasekhar (1969, p. 41). They have the form

$$D_j = g\int_0^\infty \frac{\mathrm{d}u}{\Delta\left(a_j^2+u\right)}, \tag{14}$$

where $\Delta = \sqrt{(a_1^2+u)(a_2^2+u)(a_3^2+u)}$.

For the 'thermal' terms $\Pi^{ik} \equiv \delta^{ik}\int \mathrm{d}^3x\,p - \int \mathrm{d}S_i\,x^k p$ in equation (9), we obtain

$$\Pi^{ik} = \delta^{ik}\int \mathrm{d}M\overline{\left(\frac{p}{\rho}\right)} - 4\pi g S^j_i T^k_l \bar{P}^{jl}, \tag{15}$$

where

$$\overline{\left(\frac{p}{\rho}\right)} = \frac{1}{4\pi}\int \mathrm{d}\Omega\,\frac{p}{\rho}, \tag{16}$$

and

$$\bar{P}^{jl} = \frac{1}{4\pi}\int \mathrm{d}\Omega\,pe^j_0e^l_0, \tag{17}$$

and the integration is performed over a unit sphere in Lagrangian space. Analogously, the energy term $\int \mathrm{d}^3x\,\epsilon$ in equation (8) has the form

$$\int \mathrm{d}^3x\,\epsilon = \int \mathrm{d}M\overline{\left(\frac{\epsilon}{\rho}\right)}, \tag{18}$$

where $\overline{(\epsilon/\rho)} = (1/4\pi)\int \mathrm{d}\Omega\,\epsilon/\rho$, and the surface term $\int \mathrm{d}S_i\,(pv^i)$ has the form:

$$\int \mathrm{d}S_i\,(pv^i) = 4\pi g\bar{P}^{kl}S^k_i\dot{T}^i_l. \tag{19}$$

The calculation of other terms in equations (8) and (9) is straightforward. Differentiating equation (8) with respect to M and taking into account (13), (18) and (19), we obtain

$$\frac{\mathrm{d}}{\mathrm{d}t}\left\{\frac{\dot{T}^i_n\dot{T}^i_n}{2} + 3\overline{\left(\frac{\epsilon}{\rho}\right)} - \frac{3}{2}a_j^2D_j\frac{GM}{g}\right\} = -12\pi\frac{\mathrm{d}}{\mathrm{d}M}\left\{g\bar{P}^{kl}S^k_i\dot{T}^i_l\right\} + C^i_j\dot{T}^i_lT^j_l. \tag{20}$$

Equation (20) is a differential form of the law of energy conservation. It is analogous to equation (22) of IN. Analogously, differentiating equation (9) and taking into account (12) and (15), we obtain

$$\ddot{T}^i_j = 3S^j_i\overline{\left(\frac{p}{\rho}\right)} - 12\pi S^j_k\frac{\mathrm{d}}{\mathrm{d}M} \times\left\{gS^l_iT^k_n\bar{P}^{\ln}\right\} - \frac{3}{2}A^i_ka_kD_kE^k_j\frac{GM}{g} + C^i_kT^k_j. \tag{21}$$

Equations (21) are the dynamical equations of our model. They are analogous to equations (23) of IN.

Equation (20) must follow from equations (21). To prove this, we contract both sides of equations (21) with the velocity matrix $\dot{T}^i_n$ over all indices and subtract the result from equation (20). The remainder is separated into gravitational and thermal parts. As was shown by IN, the gravitational part is reduced to the identity:

$$\frac{\mathrm{d}}{\mathrm{d}t}\left(\frac{a_j^2D_j}{g}\right) + \frac{D_ja_j\dot{a}_j}{g} = 0. \tag{22}$$

For the thermal part we have

$$\frac{\mathrm{d}}{\mathrm{d}t}\overline{\left(\frac{\epsilon}{\rho}\right)} + 3H\overline{\left(\frac{p}{\rho}\right)} + \frac{g}{\rho_0r_0^2}\bar{P}^{\ln}\dot{R}_{\ln} = 0, \tag{23}$$

where the expansion rate is defined as

$$H = \frac{1}{3}S^l_i\dot{T}^i_l = \frac{1}{3}\left(\frac{\dot{a}_1}{a_1} + \frac{\dot{a}_2}{a_2} + \frac{\dot{a}_3}{a_3}\right), \tag{24}$$

and we change variables in the last term according to the rule (11). Now we are going to prove that equation (23) follows directly from the first law of thermodynamics written in the adiabatic approximation:

$$\frac{\mathrm{d}}{\mathrm{d}t}\left(\frac{\epsilon}{\rho}\right) + p\frac{\mathrm{d}}{\mathrm{d}t}\left(\frac{1}{\rho}\right) = 0. \tag{25}$$

For that, we differentiate equations (3) and (7) with respect to time to find

$$\dot{D} = 3HD + \frac{g}{r_0^2}e_{0l}e_{0n}\dot{R}^{\ln}, \tag{26}$$

and

$$\frac{\dot{\rho}}{\rho} = -\frac{\dot{D}}{D}. \tag{27}$$

Substituting (26) and (27) into equation (25), and using (7), we obtain

$$\frac{\mathrm{d}}{\mathrm{d}t}\left(\frac{\epsilon}{\rho}\right)+3H\frac{p}{\rho}+\frac{g}{\rho_0 r_0^2}Pe_0^n e_0^l \dot{R}_{\ln}=0. \tag{28}$$

Integrating (28) over the solid angle Ω, we obtain (23). Therefore, equation (23) is equivalent to the zeroth moment of equation (25):

$$\frac{\mathrm{d}}{\mathrm{d}t}\overline{\left(\frac{\epsilon}{\rho}\right)}+\int\frac{\mathrm{d}\Omega}{4\pi}p\frac{\mathrm{d}}{\mathrm{d}t}\left(\frac{1}{\rho}\right)=0. \tag{29}$$

Now we are going to show that the quantities

$$\chi_{jk}(M)=T_k^i\dot{T}_j^i-T_j^i\dot{T}_k^i, \tag{30}$$

are exact integrals of motion of the dynamical system (21). For that, we contract the left- and right-hand sides of equations (21) with T_k^i and take the antisymmetric part of the result. We obtain

$$\dot{\chi}_{jk}(M)=12\pi g\left[\bar{P}^{\ln}\left(\delta^{kn}T_j^i\frac{\mathrm{d}}{\mathrm{d}M}S_i^l+\delta^{lj}S_\rho^k\frac{\mathrm{d}}{\mathrm{d}M}T_n^\rho-\delta^{jn}T_k^i\frac{\mathrm{d}}{\mathrm{d}M}S_i^l-\delta^{kl}S_\rho^j\frac{\mathrm{d}}{\mathrm{d}M}T_n^\rho\right)\right]. \tag{31}$$

The quantity in square brackets in (31) can be transformed to

$$\bar{P}^{nj}R^{kn}-\bar{P}^{nk}R^{jn}. \tag{32}$$

To prove that (32) is equal to zero, it is sufficient to note that both symmetric matrices $\bar{\mathbf{P}}$ and $\mathbf{R}$ can be diagonalized by the same orthogonal transformation (defined with the help of the matrix $\mathbf{O}$, see equation 6). Therefore, the commutator (32) of $\bar{\mathbf{P}}$ and $\mathbf{R}$ must be equal to zero. As was discussed by IN, the quantities $\chi_{jk}(M)$ describe the circulation of the fluid along our elliptical shells, and therefore the conservation law

$$\dot{\chi}_{jk}(M)=0 \tag{33}$$

is a direct consequence of the conservation of circulation in our model.

Let us discuss the law of conservation of angular momentum. In our model the angular momentum tensor L^{ki} can be expressed as

$$L^{ki}=\frac{1}{3}\int\mathrm{d}M\left(T_j^k\dot{T}_j^i-T_j^i\dot{T}_j^k\right). \tag{34}$$

Let the quantity l^{ki} be the angular momentum tensor density per unit of mass: $l^{ki}=\frac{\mathrm{d}}{\mathrm{d}M}L^{ki}$. Then, one can easily obtain the evolution law for l^{ki} from equations (21):

$$\dot{l}^{ki}=4\pi\frac{\mathrm{d}}{\mathrm{d}M}\left[g\bar{P}^{\ln}\left(S_k^lT_n^i-S_i^lT_n^k\right)\right]+\frac{1}{3}\left(C_n^iT_j^nT_j^k-C_n^kT_j^nT_j^i\right). \tag{35}$$

The first term in (35) describes the transfer of angular momentum between neighbouring shells arising from pressure.[4] The second term is obviously the tidal torque term. The quantity in square brackets is equal to zero in the centre and also at the boundary of the star. Therefore, if the tidal torque is absent, the angular momentum is conserved.

3 NUMERICAL WORK

For our numerical work we would like to choose a simple polytropic model of the star with the polytropic index $n=1.5$ and the specific heat ratio $\gamma=\frac{5}{3}$. The star has radius R_* and mass M_* equal to the radius and mass of the Sun. It is assumed that the star is moving along a marginally bound orbit in the field of the Kerr black hole. The same problem has been discussed by Diener et al. for the case of rather weak tidal interaction, and we use the results of this work to test our model in the relativistic tidal field. We use the natural 'stellar' units in our calculations and representation of results: the dimensionless time $\tau=t\sqrt{GM/R^3}$, the radius $\tilde{R}=r/R_*$, the mass coordinate $x=M/M_*$, energy $\tilde{E}=E*R_*/GM_*^2$ and specific angular momentum $\tilde{L}=L/\sqrt{GM_*R_*}$.

As was pointed out by IN, in the non-relativistic approximation the whole problem can be described by only two parameters: the polytropic index n, and the quantity

$$\eta_{\mathrm{nr}}=\sqrt{\frac{M_*}{M_{\mathrm{bh}}}\frac{R_{\mathrm{p}}^3}{R_*^3}}, \tag{36}$$

where M_{bh} is the black hole mass and $R_{\mathrm{p}}^{\mathrm{nr}}$ is the pericentric separation from the black hole calculated in the non-relativistic approximation. This quantity has been introduced by Press & Teukolsky (1977) in the linear theory of tidal perturbations. The smaller this quantity is, the stronger the tidal encounter will be. For the relativistic field the situation is much more complicated. For a fixed stellar model and η_{nr}, the problem must be parametrized by the ratio of the mass of the star to the black hole mass in order to specify the importance of relativistic corrections. The problem also depends on the dimensionless rotational parameter a of the black hole.[5] The orbit of the marginally bound star can be specified by its angular momentum L_{orb} and the Carter integral Q. In this paper we would like to consider the most interesting case of equatorial orbits, and therefore we set $Q=0$. We use the dimensionless orbital angular momentum $\tilde{L}_{\mathrm{orb}}=L_{\mathrm{orb}}/r_{\mathrm{g}}c$, where $r_{\mathrm{g}}=2GM_{\mathrm{bh}}/c^2$. Instead of using of η_{nr}, Frolov et al. (1994) proposed to use a more relevant quantity

$$\eta=\eta_{\mathrm{nr}}\left(R_{\mathrm{p}}/R_{\mathrm{p}}^{\mathrm{nr}}\right)^{3/2}, \tag{37}$$

where R_{p} is the minimal radial distance from the black hole calculated in the relativistic approach. Note that the corresponding dimensionless quantity $\tilde{R}_{\mathrm{p}}=R_{\mathrm{p}}/r_{\mathrm{g}}$ can be expressed only in terms of $\tilde{L}_{\mathrm{orb}}$ provided the rotational parameter a is specified.

For our calculations we use an explicit Lagrangian numerical scheme that is similar to what was used by IN. The stability criterion of our scheme is discussed in Appendix A. The essential differences of the new numerical scheme from the scheme of IN are discussed in Appendix B. The results of our calculations are presented in Figs 1–9 below.

In Figs 1–4 below we show the time dependence of different energies, the angular momentum, central density and mass lost by the star. We choose $M_{\mathrm{bh}}=1.0853\times10^7\,\mathrm{M}_\odot$, $a=0.9999$, $\eta=1.6486$ and $\tilde{L}_{\mathrm{orb}}=2.729\,45$. These parameters correspond to Diener et al.'s model 5, which has been intensely investigated in 3D finite-difference simulations. Therefore, we use this calculation for testing our model and numerical scheme. In Fig. 1 we show the time dependence of the total energy of the whole star (the upper solid curve) and the total energy of gravitationally bound debris (the lower solid curve).[6] The dot-dashed curve corresponds to the kinetic energy of the star, the dashed curve corresponds to the gravitational

[4] Note that transfer of angular momentum caused by self-gravity is absent. Obviously, this is related to our simplified description of the self-gravity forces in our model.

[5] The dimensionless rotational parameter a is determined by the black hole angular momentum J and its mass M: $a=cJ/GM^2$.

[6] The gravitationally bound debris is defined as the part of the star where the sum of kinetic and gravitational energies is less than zero.

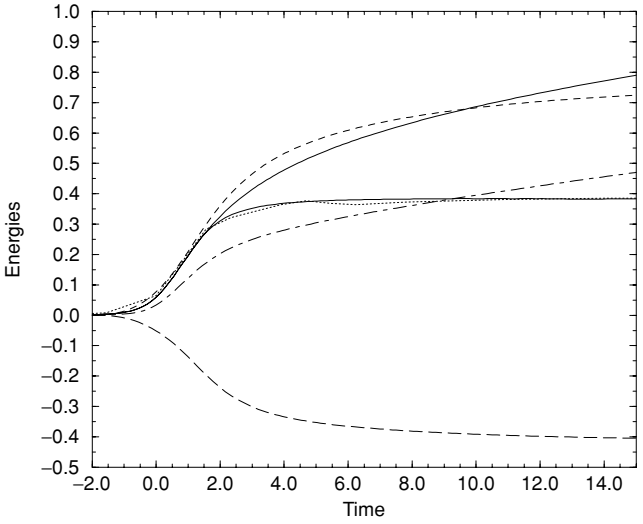

Figure 1. Evolution of total (solid curves), thermal (long-dashed curve), gravitational (short-dashed curve) and kinetic (dot-dashed curve) energies with time. All energies are measured with respect to their equilibrium values. The dotted curve represents the evolution of total energy of the gravitationally bound part of the star in the model of Diener et al.

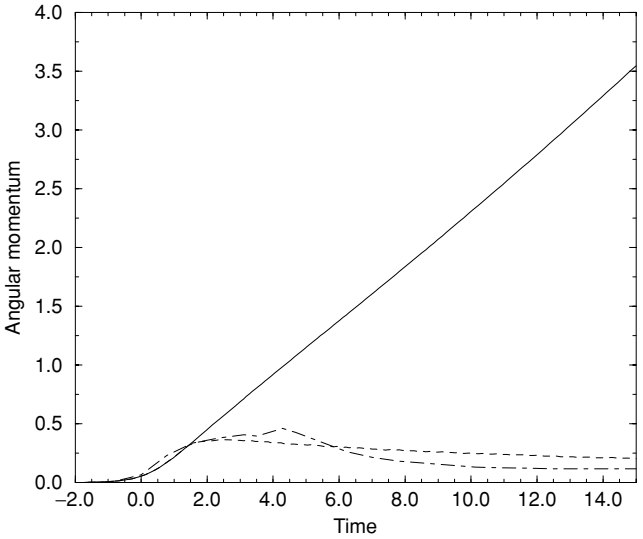

Figure 2. Evolution of the component of angular momentum perpendicular to the equatorial plane of the black hole. Solid, dashed and dot-dashed curves correspond to evolution of the total angular momentum, the angular momentum of gravitationally bound debris calculated in our model and the same quantity calculated by Diener et al., respectively.

energy of the star and the long-dashed curve corresponds to the thermal energy of the star. In general, all curves look very similar to the corresponding curves calculated by IN in the non-relativistic approximation. The dotted curve shows the time dependence of the total energy of the gravitational bound debris calculated by Diener et al. in the 3D calculations. One can see from this figure that this curve almost coincides with our curve.

In Fig. 2 the total angular momentum of the star (solid curve), the angular momentum of the gravitationally bound debris (dashed curve) and the same quantity calculated by Diener et al. (dot-dashed curve) are shown as a function of time. The total angular momentum of the star grows monotonically with time, and is significantly larger than the angular momentum of the gravitationally bound debris at the end of the calculations. The angular momentum of gravitationally bound debris calculated in the 3D simulations is close to our quantity for $\tau < 6$. Then, a sharp decrease of the angular momentum is observed and at the end of the calculation the angular momentum of Diener et al. is significantly smaller than our quantity. The reason for this behaviour of the angular momentum found in the 3D simulations is not clear to us, and therefore we cannot comment on this deviation.

In Fig. 3 the time evolution of the central density (expressed in units of the central density of the unperturbed star) is shown. The solid curve corresponds to our model and the dashed curve corresponds to the 3D simulations. We can see again that these two curves are very similar.

In Fig. 4 we show the amount of mass lost by the star (expressed in units of the stellar mass) with time. The solid curve and the dashed

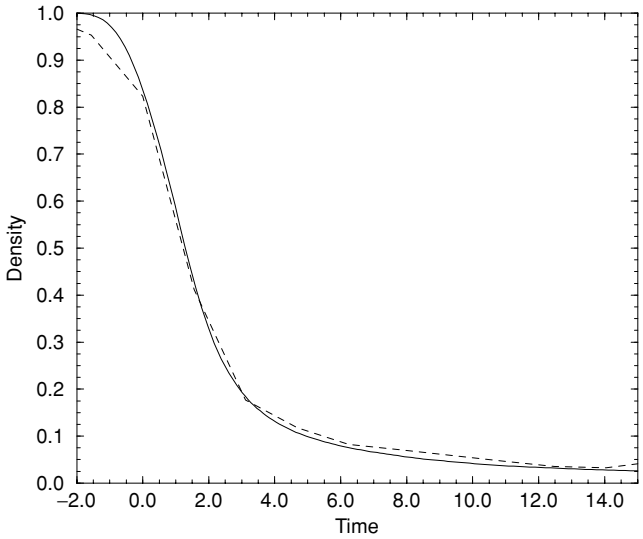

Figure 3. Evolution of the central density (expressed in units of the central density of the unperturbed star) as a function of time. The solid and dashed curves correspond to our model and the model of Diener et al., respectively.

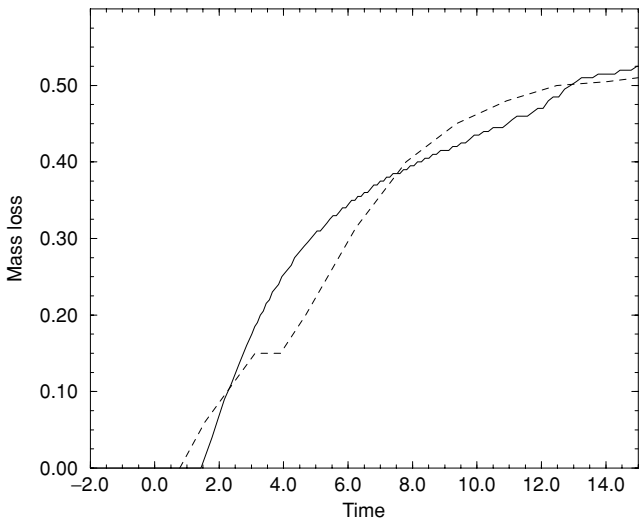

Figure 4. The amount of mass (expressed in units of the stellar mass) lost by the star during the tidal encounter as a function of time. The solid and dashed curves correspond to our model and the model of Diener et al., respectively.

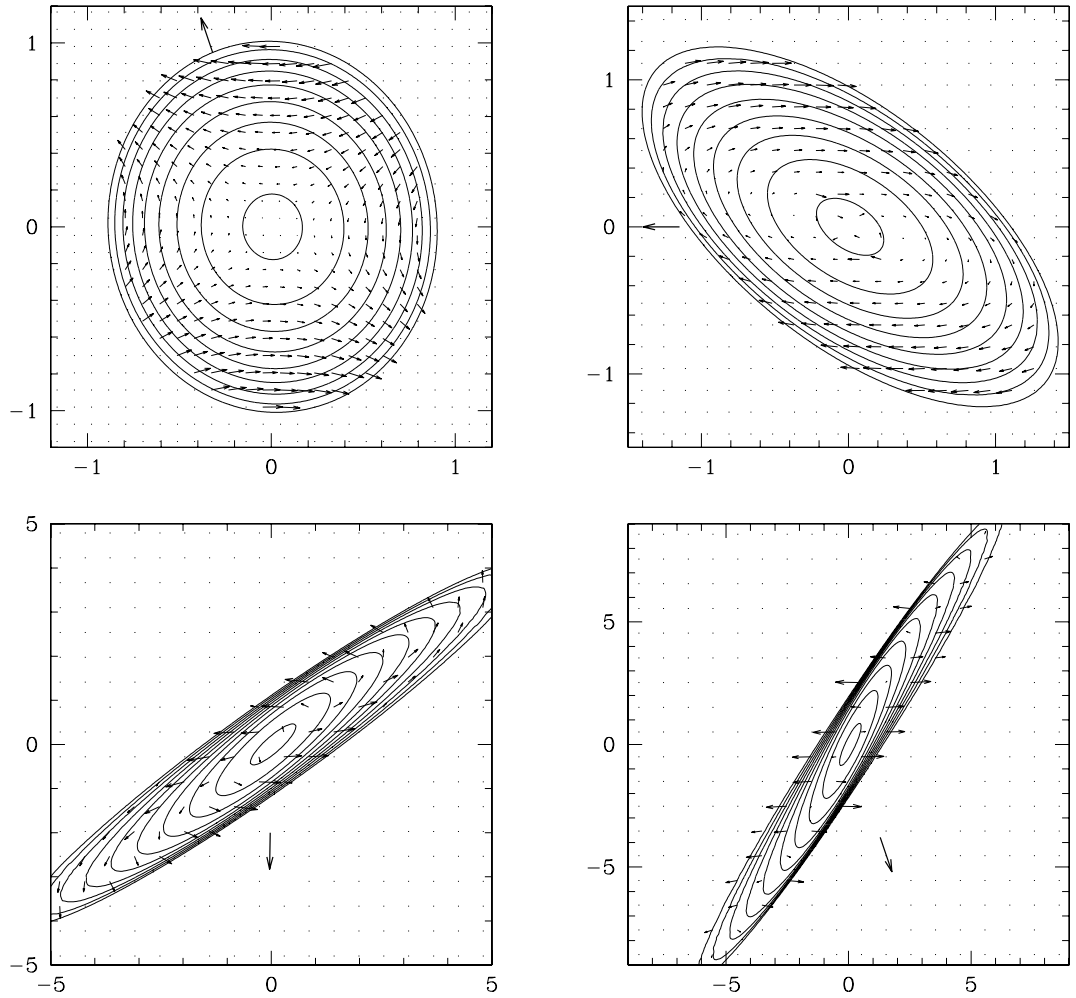

Figure 5. The time evolution of the velocity field and density contours in the orbital X–Y plane for the $\eta = 1.6486$ encounter. The spatial scales are expressed in units of the unperturbed stellar radius R_*. The large arrow points toward the black hole. The innermost contour corresponds to 95 per cent of the central density. At each subsequent contour density decreases by a factor of 1.5. Upper left-hand panel, $\tau = -2$ ($R/R_\mathrm{p} = 1.5$); upper right-hand panel, $\tau = 0$ ($R/R_\mathrm{p} = 1$); bottom left-hand panel, $\tau = 3$ ($R/R_\mathrm{p} = 1.9$); bottom right-hand panel, $\tau = 5$ ($R/R_\mathrm{p} = 2.73$). The small arrows show the direction and the relative magnitudes of the velocities.

curve correspond to our model and the 3D simulations, respectively. The asymptotic value of the mass loss is almost the same in both cases and is ~ 0.5. However, we would like to note that there is a significant ambiguity in determining the gravitationally bound gas in the 3D simulation (Diener et al.). If one considers all the gas elements that left the computational domain with velocities less than the escape velocity as still being present in the debris, the mass loss would be significantly less with an asymptotic value ~ 0.3. In general, we think that our model shows very good similarities to the 3D simulations for the parameters chosen in this computation.

Fig. 5 shows the time evolution of the velocity field and density contours in the orbital (XOY) plane for the same model. Axis (OX) is directed opposite to the black hole during the pericentre passage. Time $\tau = 0$ corresponds to the time of the pericentre passage. In this figure one can see that the density contours lose their spherical shape with time and elongate. The size of the outermost contour at $\tau = 5$ is approximately 10 times larger than at $\tau = -2$. In the beginning, the contours expand in the direction of the black hole, but as the star approaches the pericentre of its orbit, they start to lag behind. The lag of the innermost contours is slightly less than that of the outer ones. The distribution of the velocities in the star is represented by arrows, the lengths of which are proportional to the velocity magnitude.

Now let us discuss some simple properties of the parameter space of the problem. Figs 6–9 below show dependences of the mass lost by the star, the total energy contained in the gravitationally bound debris and the angular momentum of the debris on the orbital angular momentum $\tilde{L}_\mathrm{orb}$ for two values of the rotational parameter of the black hole: $a = 0.9999$ and 0. The mass of the black hole and other orbital parameters are the same as in the previous calculations. The largest orbital angular momentum corresponds to $\eta = 2$, the smallest angular momentum corresponds to the total disruption of the star (we denote the respective value of η as the 'critical' value η_cr).

Figs 6 and 7 show the dependence of the mass lost by the star on the absolute magnitude of the orbital angular momentum and parameter η, respectively. The solid and dashed curve correspond to positive and negative angular momenta and are calculated for $a = 0.9999$. The dotted curve is calculated for $a = 0$. It is seen from the figures that the stars with negative orbital angular momenta are disrupted much more effectively than the stars with positive angular

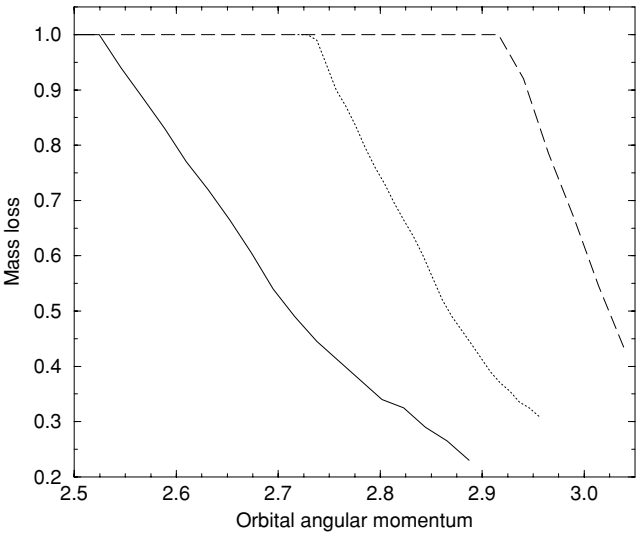

Figure 6. The mass lost by the star after a fly-by of the black hole is shown as a function of the absolute magnitude of the dimensionless orbital momentum. The case $M_{\rm bh} = 1.0853 \times 10^7\,{\rm M}_\odot$ is considered. The solid and dashed curves correspond to $a = 0.9999$, positive and negative orbital angular momenta, respectively. The dotted curve correspond to $a = 0$.

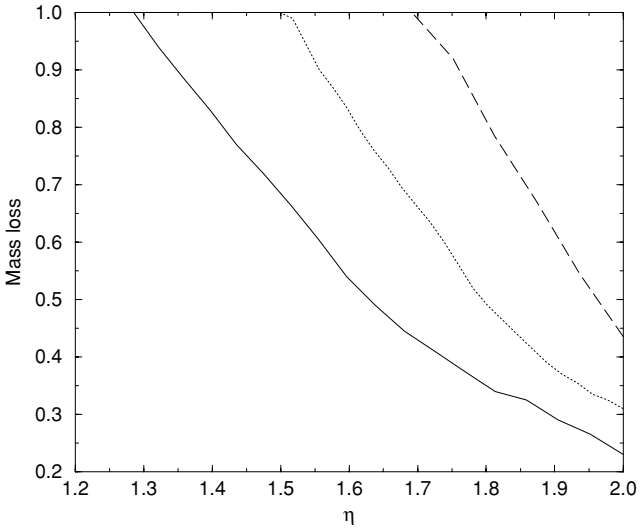

Figure 7. Same as Fig. 6, but the mass lost by the star is shown as a function of the parameter η.

momenta.[7] It is obvious that similar curves calculated for smaller rotational parameters of the black hole (but with the same mass) must lie between the solid and dashed curves. We have $\eta_{\rm cr} = 1.5$ for $a = 0$ and $\eta_{\rm cr} = 1.28,\ 1.69$ for $a = 0.9999$ and positive and negative orbital angular momenta, respectively.

In Fig. 8 we show the dependence of the total energy of the gravitationally bound debris calculated after the fly-by of the black hole on the value of the dimensionless orbital angular momentum. Similarly to Figs 6 and 7 representing the mass loss, Fig. 8 shows that the stars moving on orbits with negative orbital angular momentum are perturbed more effectively than the stars moving on orbits with

[7] Note that this effect has been discussed by Beloborodov et al. (1992) within the framework of a rather naive criterion for tidal disruption.

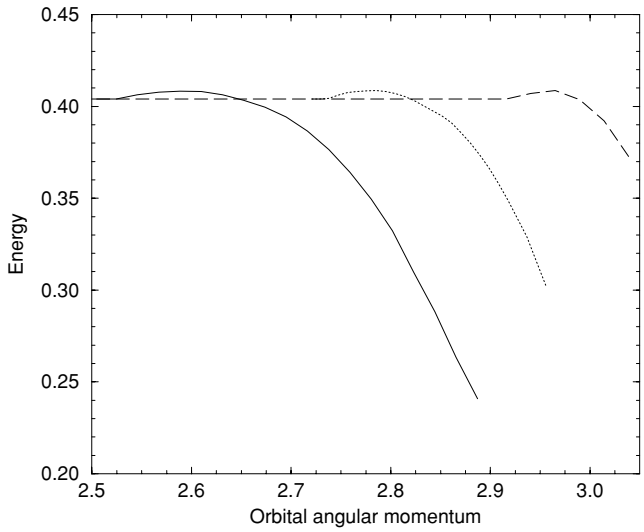

Figure 8. The energy of gravitationally bound debris is shown as a function of the absolute magnitude of the dimensionless orbital angular momentum. The solid and dashed curves correspond to $a = 0.9999$, positive and negative orbital angular momenta, respectively. The dotted curve correspond to $a = 0$

positive angular momentum. It is interesting to note that the asymptotic value of the total energy in the limit of small orbital angular momentum (corresponding to full disruption of the star) is a non-zero quantity that depends neither on the spin of the black hole nor on the sign of the orbital angular momentum (see Fig. 8). This could be explained as follows: after the fly-by the stellar gas leaves the star with almost zero specific total energy (i.e. parabolic velocities). So, the out-flowing gas carries virtually no specific energy, and the energy of the gravitationally bound part of the star is conserved. In Fig. 9 we show the component of the angular momentum of the star perpendicular to the orbital plane after the fly-by as a function of the dimensionless orbital angular momentum. In contrast to the total energy, the angular momentum of the gravitationally bound debris

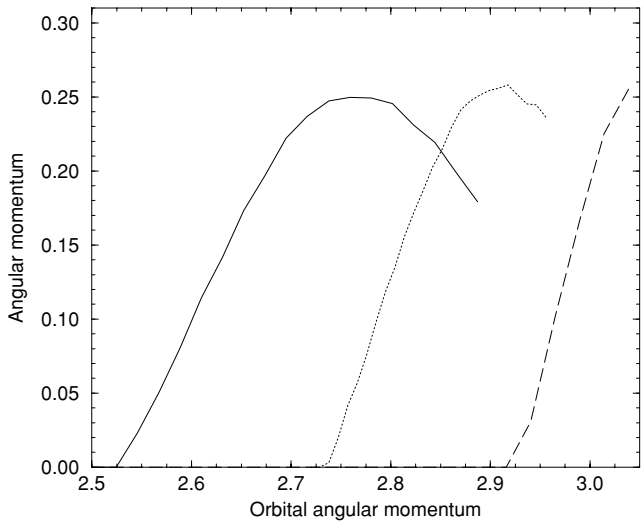

Figure 9. The angular momentum of gravitationally bound debris is shown as a function of the absolute magnitude of the dimensionless orbital angular momentum. The solid and dashed curves correspond to $a = 0.9999$, positive and negative orbital angular momenta, respectively. The dotted curve corresponds to $a = 0$.

is a non-monotonic function of the dimensionless orbital angular momentum.

4 DISCUSSION

In this paper we construct a self-consistent variant of the new model of a tidally perturbed or tidally disrupted star proposed by Ivanov & Novikov (2001). The model allows researchers to calculate the outcome of the tidal disruption event with the help of a one-dimensional Lagrangian numerical scheme. Therefore, it is much faster than the conventional numerical 3D approach, and it could be evolved for a much longer time. We use the model in numerical calculations of the tidal interaction of an $n = 1.5$ polytropic star with a Kerr black hole of mass $10^7\,M_\odot$. We compare the results of our calculations with the results of finite-difference 3D calculations of the same problem and find a very good agreement between them. Then, we consider dependences of the main characteristics of the tidally perturbed star after a fly-by of the black hole in the equatorial plane on the value of the orbital angular momentum. We find that the stars with negative orbital angular momentum are perturbed more effectively than stars with positive orbital angular momentum. We also briefly discuss the dependence of the outcome of the tidal encounter on the spin of the black hole.

As was demonstrated in the present work (see also IN), the model gives results that in certain cases coincide almost completely with results of 3D calculations. On the other hand, the dynamical equations of our model cannot be reduced to the exact hydrodynamical equations. Therefore, a natural question arises: why is the agreement between the two approaches so good? The possible explanation might be as follows. The key assumption of our model consists in using elliptical shells for the description of the shape of the star evolving under the influence of the tidal field. It seems that the quadrupole dependence of the field of tidal forces on the angular coordinates and the special algebraic properties of the tidal tensor could justify such assumptions at least for large-scale hydrodynamical motions induced in the star. This could answer qualitatively the question of why different elements of the star that are not in causal contact evolve in such a way that the elliptical form of the shells is always maintained.

Now let us discuss the problems of our model. At first we discovered in our numerical calculations that our numerical scheme is slowly unstable for stellar models with a sharper density contrast. For example, in the case of an $n = 3$ polytrope it takes several characteristic 'stellar' times for the instability to halt the computations. Since our numerical scheme has been written in a rather naive manner, we expect that a more sophisticated numerical scheme (e.g. an implicit scheme) could resolve this difficulty.

There is a more fundamental problem with our model. We managed to obtain the distribution of pressure and density across the star in a simple form only for a polytropic star. Therefore, it is not clear to us how to generalize our model directly for the case of a more realistic stellar gas.[8] However, the general properties of the tidal disruption of a more realistic star can be understood qualitatively in the following way. It is well known that the low-mass stars are fully convective, and therefore they can be modelled by the $n = 1.5$ polytrope. Therefore, our results are qualitatively valid for such stars. On the other hand, the high-mass stars are closer to the $n = 3$ polytrope. For a given η, the higher polytropic index is, the more concentrated towards the centre the stellar model will be, and a stronger tidal field will be needed in order to disrupt such a star (see also IN). The next step to a more realistic model could be to consider a two-layer model, with two different polytropic indices for the stellar interior and stellar envelope. Such a consideration could account for the presence of a radiative core and a convective envelope (or a convective core and a radiative envelope). A generalization of our model to the case of non-adiabatic stars could also be made. For example, it is possible to introduce a term accounting for energy release arising from nuclear reactions in the differential form of the energy conservation equation (equation 23, see also e.g. Carter & Luminet 1983).

In the present paper we do not make an attempt to comprehensively survey the parameter space of the relativistic tidal problem and to calculate cross-sections of a different kind. This will be treated in future work.

[8] Note that the variant of the model considered by IN is free from this difficulty.

ACKNOWLEDGMENTS

We are grateful to J. C. B. Papaloizou and A. G. Polnarev for very useful discussions, and Martin Goetz for very helpful comments. This work has been supported in part by RFBR grant 00-02-16135, in part by the Danish Research Foundation through its establishment of the Theoretical Astrophysics Center, and in part by the Danish Natural Science Research Council through grant no 9701841.

REFERENCES

Beloborodov A.M., Illarionov A.F., Ivanov P.B., Polnarev A.G., 1992, MNRAS, 259, 209
Carter B., Luminet J.-P., 1982, Nat, 296, 211
Carter B., Luminet J.-P., 1983, A&A, 121, 917
Carter B., Luminet J.-P., 1985, MNRAS, 212, 23
Chandrasekhar S., 1969, Ellipsoidal Figures of Equilibrium. Yale Univ. Press, New Haven
Diener P., Frolov V.P., Khokhlov A.M., Novikov I.D., Pethick C.J., 1997, ApJ, 479, 164
Frolov V.P., Khokhlov A.M., Novikov I.D., Pethick C.J., 1994, ApJ, 432, 680
Ivanov P.B., Novikov I.D., 2001, ApJ, 549, 467 (IN)
Lattimer J.M., Schramm D.M., 1976, ApJ, 210, 549
Press W.H., Teukolsky S.A., 1977, ApJ, 213, 183

APPENDIX A: PROPAGATION OF SMALL PERTURBATIONS AND THE TIME-STEP CONSTRAINT

In a standard approach the time-step constraint must follow from a stability analysis of numerical schemes. However, the standard stability analysis of our numerical scheme is rather complicated and therefore we do not use it in our paper. Following IN, we constrain our time-step by the condition

$$\delta t = \frac{\alpha \delta M}{c_{\mathrm{s\,max}}}. \tag{A1}$$

Here $\alpha < 1$ is a parameter. $c_{\mathrm{s\,max}}$ is greater than or equal to the velocity of propagation of a small perturbation (with respect to the mass coordinate) c_{s} calculated in the analytical linear approximation: $c_{\mathrm{s\,max}} \geqslant c_{\mathrm{s}}$. For the stellar gas we assume the equation of state of an ideal gas with polytropic index γ.

To estimate $c_{\mathrm{s\,max}}$ we decompose our dynamical variable $\mathbf{T}$ into a background part and a perturbation: $\mathbf{T} = \mathbf{T}_0 + \mathbf{t}$, where the perturbation $\mathbf{t}$ is assumed to be of standard oscillatory form

$$\mathbf{t} = \tilde{\mathbf{t}} \mathrm{e}^{\mathrm{i}(\omega t + kM)}. \tag{A2}$$

For the velocity c_s we have

$$c_s = \frac{\omega}{k}.$$

The dynamical equation for the perturbation follows directly from equations (21) and (17). Neglecting the dependence of the background quantities on the mass coordinate and taking into account only the second term on the right-hand side of equation (21), we have:

$$\frac{\partial^2}{\partial t^2} t^i_j = 24\pi^2 \gamma g^{(1-\gamma)} r_0^{2(\gamma+1)} p_0 \rho_0 S^l_i H^{ljkn} \times \left(S^k_m \frac{\partial^2}{\partial M^2} t^m_n + S^n_m \frac{\partial^2}{\partial M^2} t^m_k \right), \tag{A3}$$

with the symmetric tensor

$$H^{ljkn} = \int \frac{\mathrm{d}\Omega}{4\pi} \frac{e^l_0 e^j_0 e^k_0 e^n_0}{\left(e^s_0 e^\rho_0 R^\rho_s\right)^{(\gamma+1)}}. \tag{A4}$$

Substituting (A2) in (A4), one can obtain a set of algebraic equations. Then, the usual compatibility condition gives the value of the velocity c_s. However, this is too complicated for our purposes. To estimate the upper limit of the velocity, we can use an upper limit estimate for the tensor H^{ljkn}:

$$H^{ljkn} \leqslant \frac{1}{15 f_{\min}} (\delta^{lj}\delta^{kn} + \delta^{lk}\delta^{\ln} + \delta^{\ln}\delta^{lk}), \tag{A5}$$

where $f_{\min}$ is the minimal eigenvalue of the matrix $\mathbf{R}$. Substituting (A5) in (A3), and using (A2), we have

$$a^l_j = \frac{A}{c_s^2} S^l_i S^k_i \left(a^j_k + a^k_j + \delta^k_j a^n_n \right), \tag{A6}$$

where

$$a^l_j = S^l_i \tilde{t}^i_j, \tag{A7}$$

and

$$A = \frac{(4\pi)^2}{5} \gamma g^{(1-\gamma)} \frac{r_0^{2(\gamma+1)}}{f_{\min}^{\gamma+1}} p_0 \rho_0. \tag{A8}$$

Let us assume the matrix $\mathbf{a}$ to be symmetric: $\mathbf{a} = \mathbf{a}^{\mathrm{T}}$. In this case both matrices a^l_j and $S^l_i S^j_i$ can be diagonalized by the same transformation. Taking into account that the quantities a_i^{-2} are the eigenvalues of the matrix $S^l_i S^j_i$, equation (A6) can be reduced to the form

$$c_i = \frac{A}{c_s^2} a_i^{-2} \left(2c_i + \sum_{i=1}^{i=3} c_i \right), \tag{A9}$$

where the quantities c_i are the eigenvalues of the matrix $\mathbf{a}$. Equation (A9) has non-trivial solutions if and only if

$$1 = \sum_{i=1}^{i=3} \frac{1}{\left(a_i^2 x - 2\right)}, \tag{A10}$$

where $x = c_s^2/A$. Obviously, equation (A10) gives an implicit dispersion relation. A simple analysis of equation (A10) shows that all roots of (A10) are larger than

$$f = 3\left(\frac{1}{a_1^2} + \frac{1}{a_2^2} + \frac{1}{a_3^2} \right), \tag{A11}$$

and we have

$$c_s > \sqrt{fA}. \tag{A12}$$

Therefore, we use the condition

$$\delta t = \frac{\alpha \delta M}{\sqrt{fA}} \tag{A13}$$

in order to constrain our time-step.

APPENDIX B: THE NUMERICAL SCHEME

The numerical scheme used in the computations is very similar to what was used by IN and we address the reader to Appendix B of IN for a comprehensive description of the scheme. The main difference is determined by the fact that we now calculate the exact distributions of pressure and density across the star, in contrast to the approximate treatment of these quantities by IN. These quantities determine the thermal terms, (16) and (17), which in turn determine the action of pressure forces in our model. In this Appendix we outline the numerical evaluation of the thermal terms, (16) and (17).

The calculation of these terms can be subdivided into two steps. First, with the help of a special subroutine we find the eigenvalues and eigenvectors of the shear matrix $\mathbf{R}$ (i.e. the quantities f_m and the matrix $\mathbf{O}$, see equation 6). The pressure tensor (17) is diagonal in the frame of eigenvectors of the matrix $\mathbf{R}$. Therefore, we have to evaluate numerically only four quantities: three eigenvalues of the tensor (17) and the quantity (16). It turns out that in the case of a polytropic stellar gas, the eigenvalues of the pressure tensor are proportional to the following integrals:

$$I_i \equiv \int_0^{2\pi} \mathrm{d}\phi \int_0^{\pi} \mathrm{d}\theta \sin(\theta) \times \frac{e_i^2}{\left\{ f_1 \cos^2(\theta) + \sin^2(\theta)\left[f_2 \cos^2(\theta) + f_3 \sin^2(\theta) \right] \right\}^{\gamma}}, \tag{B1}$$

where e_i are the direction cosines and $\gamma = \frac{5}{3}$ is the specific heat ratio. The quantity (16) is proportional to

$$I_0 \equiv \int_0^{2\pi} \mathrm{d}\phi \int_0^{\pi} \mathrm{d}\theta \sin(\theta) \times \frac{1}{\left\{ f_1 \cos^2(\theta) + \sin^2(\theta)\left[f_2 \cos^2(\theta) + f_3 \sin^2(\theta) \right] \right\}^{\gamma-1}}. \tag{B2}$$

Integrals (B1) and (B2) are evaluated numerically by a separate program and tabulated as functions of the ratios $f(2)/f(1)$ and $f(3)/f(1)$. For small and large values of the ratios we use analytical representations of these integrals in terms of series.

This paper has been typeset from a TEX/LATEX file prepared by the author.